Luminescence Properties of CsPbBr3:Mn

**Nanocrystals** 

Wencai He, Qiqi Zhang, Yifang Qi, Jian Xiong, Paresh Ray, Nihar Ranjan Pradhan, Tigran V.

Shahbazyan, Fengxiang Han, and Qilin Dai\*

Department of Chemistry, Physics, and Atmospheric Sciences, Jackson State University, Jackson,

MS, 39217, United States

\*corresponding author: qilin.dai@jsums.edu

KEYWORDS: CsPbBr<sub>3</sub>, energy transfer, luminescence, photodetector, Mn

Abstract

Mn doped CsPbBr<sub>3</sub> nanocrystals with sizes of ~10 nm are synthesized by hot injection method via

the addition of HBr in the precursor. The sizes and crystal structure are not influenced by the

addition of HBr. The photoluminescence (PL) mechanism of CsPbBr<sub>3</sub> is modified by HBr, leading

to the PL peak shift to 433 nm, which is not the regular PL of CsPbBr<sub>3</sub>. The irregular CsPbBr<sub>3</sub>

nanocrystals prepared with HBr enable the Mn doping, leading to the red emission of Mn. The PL

energy transfer from CsPbBr<sub>3</sub> to Mn is studied as a function of HBr. The energy transfer of ~90%

is achieved in this system. In addition, The crystallinity of the CsPbBr3 nanocrystals is also

improved by the HBr, leading to better photodetector device performance.

1

#### Introduction

CsPbBr<sub>3</sub> nanocrystals are attracting much attention due to their applications in optoelectronic devices, lighting and displays, etc.[1–27] Green PL properties from CsPbBr<sub>3</sub> nanocrystals due to CsPbBr<sub>3</sub> exciton emission are commonly reported, which shows significant potential in green lighting devices. Mn ions as red PL centers due to the transition from <sup>4</sup>T<sub>1</sub> to <sup>6</sup>A<sub>1</sub> are extensively studied.[28] Mn doped inorganic perovskite CsPbCl<sub>3</sub> nanocrystals have been reported by many papers.[29-37] Efficient PL energy transfer from CsPbCl<sub>3</sub> to Mn is proposed, leading to blue emission from CsPbCl<sub>3</sub> and red emission from Mn.[38] However Mn doped CsPbBr<sub>3</sub> are only reported by Pradhan et al. [39] and Son et al. [40] In Pradhan's results, Mn doped CsPbBr<sub>3</sub> are synthesized by adopting a self-regulated approach and the PL depends on the concentration of the solution. Low concentration produces CsPbBr<sub>3</sub> dominate PL. High concentration yield Mn dominates PL. Therefore, the PL of CsPbBr<sub>3</sub> prepared by this method is not as stable as that of CsPbCl<sub>3</sub>. Son developed Mn doping method by HBr additive.[40] Very strong red emission from Mn were produced in their method. However, the green emission is missing in their paper. A peak at ~440 is observed due to the units of PbBr6 octahedra in the thickness corresponding to ~2 nm in CsPbBr<sub>3</sub> nanoplatelets.[40,41] The energy transfer between CsPbBr<sub>3</sub> and Mn is not studied, and the reason for the successful Mn doping in CsPbBr<sub>3</sub> is still not clear.

In this work, Mn doped CsPbBr<sub>3</sub> in the presence of HBr are synthesized based on modified Son's method.[40] The sizes and crystal structures of the CsPbBr<sub>3</sub> are not influenced by the HBr additive, However, the PL peak shift to 433 nm, leading to the irregular PL of CsPbBr<sub>3</sub>. The irregular PL leads to the Mn doping in CsPbBr<sub>3</sub>, resulting in energy transfer from CsPbBr<sub>3</sub> to Mn to produce red emission. The energy transfer is significantly influenced by the amount of HBr and

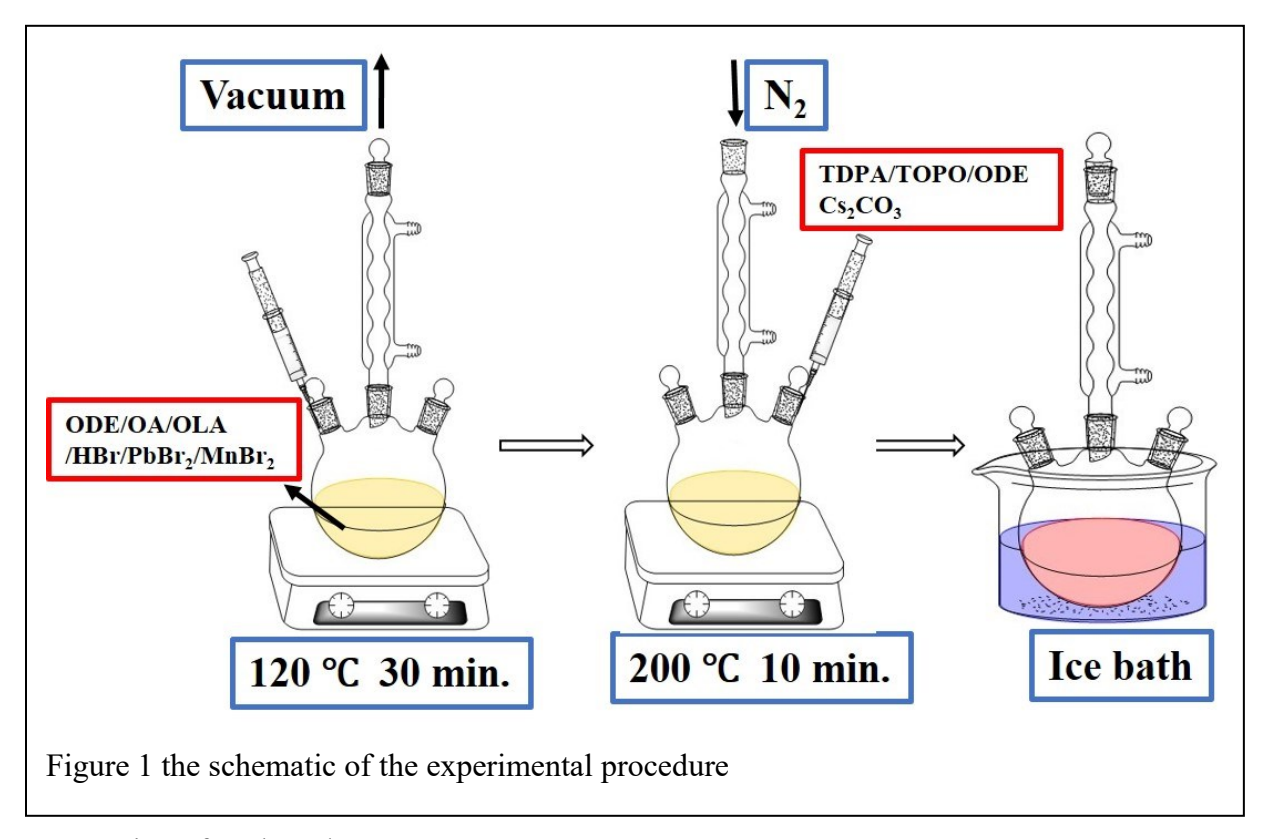
is studied in terms of energy transfer efficiency by Time-resolved PL (TRPL) spectra affected by HBr. In addition, the photodetectors based on the doped and undoped CsPbBr<sub>3</sub> are studied for comparison. The Mn doped CsPbBr<sub>3</sub> nanocrystals exhibit better performance compared to the undoped CsPbBr<sub>3</sub> nanocrystals.

## Experimental

#### Chemicals and materials

Manganese bromide hydrate 98%, cesium carbonate 99.9%, lead (II) bromide 99.998%, oleic acid 90% (OA), and n-Tetradecylphosphonic acid 98% (TDPA) were purchased from Alfa Aesar. Hydrobromic acid 48% solution in water was purchased from Acros Organics. Trioctylphosphine oxide 90% (TOPO) was purchased from Sigma Aldrich. Oleylamine (OLA) was purchased from TCI America.

The method used in this work is based on Son's method.[40] Typically, Cs solution was injected into PbBr<sub>2</sub> and MnBr<sub>2</sub> solution at 200 °C. Figure 1 shows the schematic of the experimental procedure. Table 1 shows the sample information and sample names in this work.



# Preparation of Cs-based precursor

0.0317 g TDPA, 0.5438 g TOPO, 0.0091 g Cs<sub>2</sub>CO<sub>3</sub> were loaded in a 100 ml three-neck round-bottom flask, and then the mixture was degassed 3 times and kept vacuum for 30 min at room temperature. 4 ml ODE was injected into the flask and kept vacuum for 10 min at room temperature. The mixtures were heated to 120 °C under vacuum for 30 min to obtain a clear solution. Then the solution was heated to 230 °C under N<sub>2</sub> for the next step.

## Synthesis of CsPbBr<sub>3</sub>:Mn

0.7 ml OLA and HBr (0-1 ml) were mixed in a 25 ml three-neck round-bottom flask under N<sub>2</sub> for 2 min, then transferred to vacuum, and kept for 10 min. 5 ml ODE and 0.7 ml OA were injected into the flask under N<sub>2</sub>. 0.0587 g PbBr<sub>2</sub>, 0.1696 g MnBr<sub>2</sub> were put in the flask, and then were degassed 3 times, then the solution was kept under vacuum for 30 mins at room temperature. The mixtures were kept at 120 °C under vacuum for 1h. Then the solution was heated to 200 °C under

N<sub>2</sub>. Additional 0.7 ml OA and 0.7 ml OLA were injected into the solution when the temperature reached 200 °C. After 10 min, 4.5 ml Cs-based precursor was injected into the above solution. After 1 min, the flask was cooled in an ice bath to obtain CsPbBr<sub>3</sub>:Mn nanoparticles. The nanoparticles were dispersed in toluene for PL measurements. Table 1 shows the sample information in terms of the amount of MnBr<sub>2</sub> and HBr during the sample synthesis.

Table 1 the sample information in this work

Sample name	MnBr <sub>2</sub> / g	HBr/ mL
S1	0	0
S2	0	0.2
S3	0.1696	0.2
S4	0.1696	0.4
S5	0.1696	0.6
S6	0.1696	0.8
S7	0.1696	1.0

#### Characterization

The morphology of nanocrystals was measured by a transmission electron microscope (TEM) (JEM-1011, JEOL). The crystallinity and phase of the CsPbBr<sub>3</sub>:Mn materials were studied by an X-ray diffraction system (XRD) (MiniFlex 600, Rigaku). PL spectra were collected by Horiba fluoromax-4 Compact Spectrofluorometer. Time-resolved PL (TRPL) spectra were obtained with fluorescence spectrophotometer (FluoroMax, Horiba) with TCSPC accessories under 370 nm light excitation.

## Results and discussion

Figure 2a shows the XRD diffraction patterns of the CsPbBr<sub>3</sub> samples S1-S3. Mn doping and HBr additive don't affect the CsPbBr<sub>3</sub> crystal phase. XRD diffraction patterns of S1, S2, and S3 are consistent with the Son' results.[40] The **XRD** diffraction peaks at 15.2°, 21.5°, 30.4°, and 34.3° are indexed to (100), (110), (200), and (210)

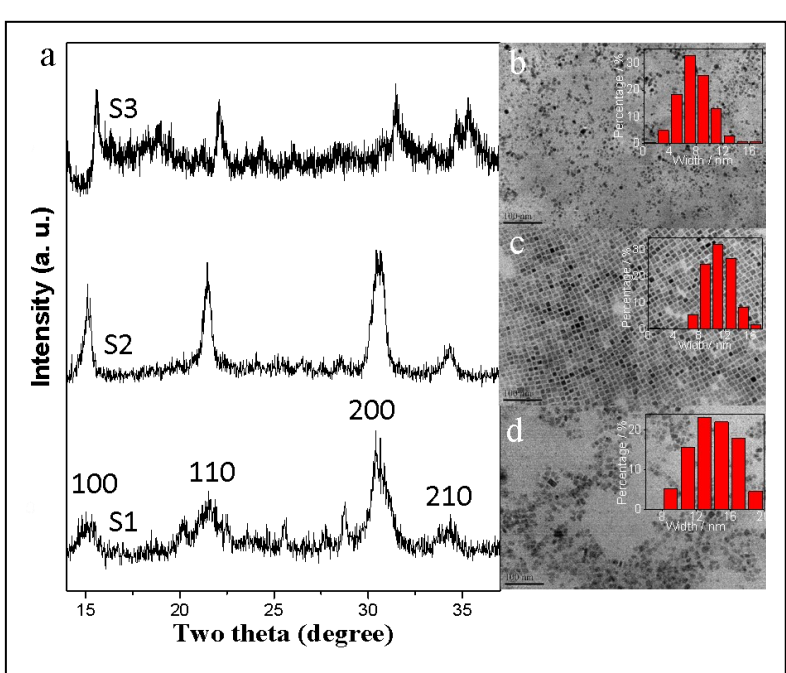


Figure 2 XRD diffraction patterns of S1, S2 and S3 and corresponding TEM images. The insets show the size distribution.

crystal planes. [42] It shows that the peaks of the Mn-doped CsPbBr<sub>3</sub> S3 are narrower compared to those of the undoped samples (S1 and S2), indicating the improved crystallinity by Mn doping. In addition, it can be observed that the diffraction peaks of S3 shift to large-angle side compared to the two undoped samples S1 and S3. This is explained by Mn doping, which is consistent with

Son's results.[40] Figure 2b, c, and d show the TEM images of S1, S2, and S3, respectively. The particle size distributions of the three samples are shown in the insets of figure b, c and d. The average sizes of the three samples are 8 nm, 10 nm, and 13 nm for S1, S2, and S3, respectively. Therefore, the average sizes of the three samples are ~10 nm. Thus, the Mn doping and HBr additive cannot affect the sizes and the structure of the nanoparticles.

The effects of HBr additive and Mn doping on the PL properties are investigated, and the emission and excitation spectra of S1-S7 are shown in figure 3. Figure 3a shows the PL spectrum

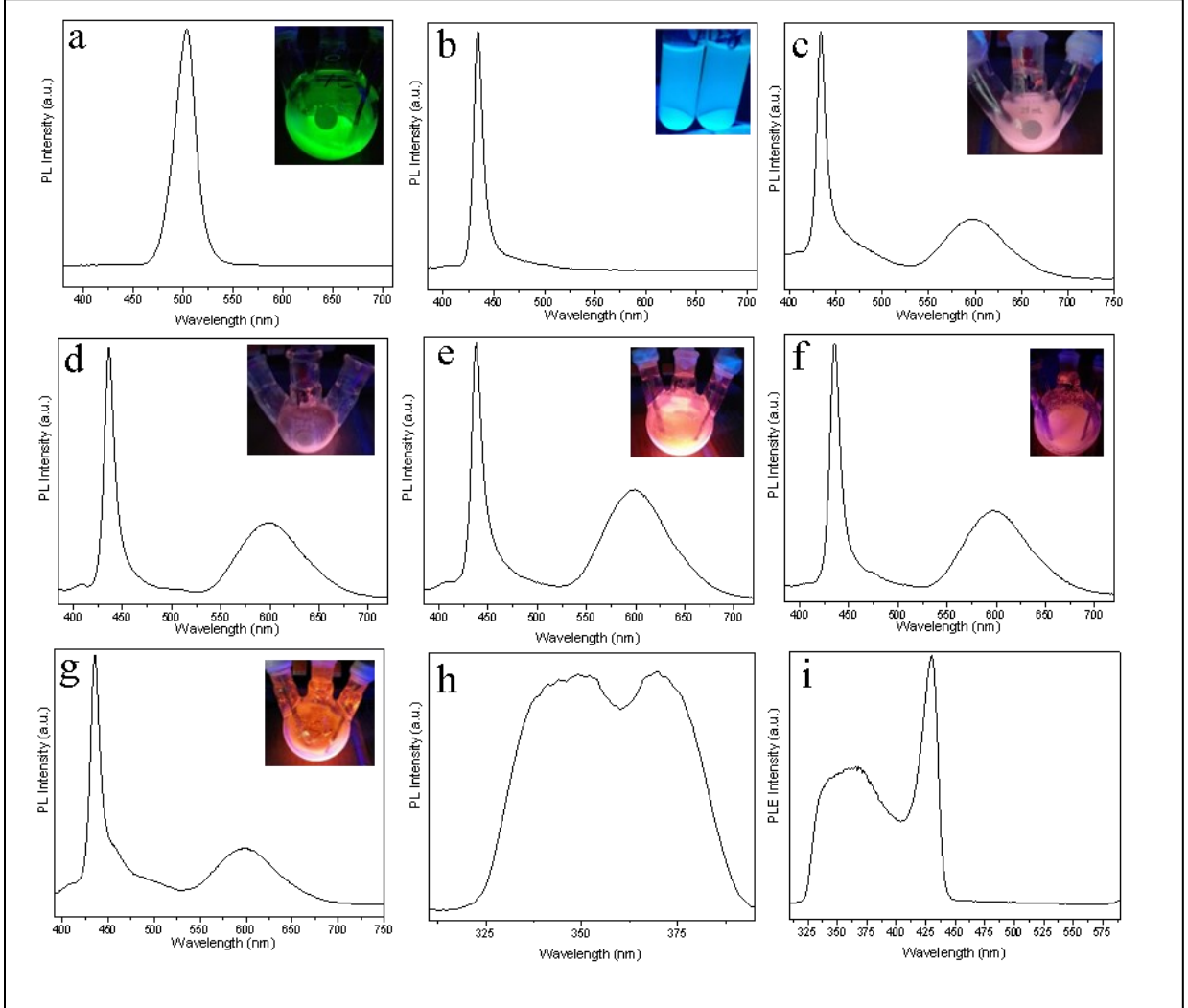


Figure 3 a-g PL spectra of S1-S7 ( $\lambda_{ex}$ =365 nm). h PLE spectra of S2 monitored at 433 nm. i PLE spectra of S3 monitored at 600 nm.

of S1 with a peak at 503 nm, which is attributed to exciton emission. It is a very typical PL spectrum of CsPbBr<sub>3</sub>, which is consistent with the literature report about CsPbBr<sub>3</sub> emission.[26,43] Figure 3b shows the emission spectrum of S2 with a peak at ~433 nm, which is different compared with that of S1. It can be seen that the HBr additive leads to the PL emission peak shifts from 503 nm to 433 nm. It suggests that the addition of HBr affects the PL mechanism of CsPbBr<sub>3</sub> although the XRD different patterns and sizes of the particles are not influenced by HBr (Fig. 2). It is reported that the 433 nm is attributed to the three units of PbBr<sub>6</sub> octahedra in the thickness corresponding to ~2 nm.[40,41] The significant blueshift is due to the 1-dimensional quantum confinement in nanoplatelets.[40,41] The amount of HBr increases from 0.2 mL to 1.0 mL for samples S3-S7 as indicated in table 1. Two PL peaks are observed for S3-S7 including 433 nm from CsPbBr<sub>3</sub> and ~600 nm from Mn (Fig.3 c-g), which is consistent with Son's results. Mn PL peak is attributed to the  ${}^4T_1 \rightarrow {}^6A_1$  transition.[28] The presence of 600 nm PL peak indicates the successful Mn doping in CsPbBr<sub>3</sub> crystal lattice. It can be seen that the relative Mn PL intensity to CsPbBr<sub>3</sub> PL intensity is significant influenced by the amount of HBr. The insets of figure 3a-g show the corresponding photographs of the samples under the UV lamp. Bright green, pink, or red emissions can be observed. The PLE spectra of S2 is shown in figure 3h ( $\lambda_{em}$ =433 nm). A broad absorption band in the range of 320-400 nm is observed, indicating that the absorption of the energy at the range of 320-400 nm corresponds to the emission of 433 nm. Therefore, the broad absorption is attributed to the CsPbBr<sub>3</sub> matrix. PLE spectra of S3-S7 look identical to each other, and the PLE spectrum of S3 is exhibited in figure 3i ( $\lambda_{em}$ = 600 nm). Two components are observed in the spectrum. A broad band 320-400 nm is assigned to the CsPbBr<sub>3</sub> matrix absorption since it is similar to the PLE spectrum in figure 3h. Therefore, Mn emission can be realized by energy transfer from CsPbBr3 matrix absorption. The other peak is located at 430 nm, which is attributed

to PbBr6 octahedra. PbBr<sub>6</sub> octahedra has an emission of 433 nm peak, and the absorption is highly possible to be 430 nm sharp peak. Another energy transfer from PbBr<sub>6</sub> octahedra in CsPbBr<sub>3</sub> to Mn, leading to red emission of Mn. Therefore, the PLE spectrum of S3 shows that energy transfer happened from CsPbBr<sub>3</sub> to Mn by two channels, leading to the Mn red emission at ~600 nm. Two energy transfer channels are provided by the CsPbBr<sub>3</sub>. One channel is due to the PbBr<sub>6</sub> octahedra absorption. The other channel is attributed to CsPbBr<sub>3</sub> matrix absorption. Figure S1 shows the PL spectra of S3 under the excitation of 433 nm. It can be seen that 600 nm PL peak is also observed in the spectrum, indicating the energy transfer from PbBr<sub>6</sub> octahedra to Mn. Figure S2 shows the PLE spectrum of S1, which is different from that of S2, indicating the modified PL mechanism by HBr. Figure S3 shows the energy transfer mechanism in our CsPbBr<sub>3</sub>:Mn nanocrystals. CsPbBr<sub>3</sub> matrix absorbs the energy and the energy will be transferred to Mn (Channel 1). PbBr<sub>6</sub> octahedra absorbs the energy and then transfer to Mn (Channel 2). Channel 2 is more efficient because the intensity of 430 nm peak is higher than that of the broad band. There are no reports about the Mn ion doping in CsPbBr<sub>3</sub> nanocrystals with the PL peaks of 503 nm from CsPbBr<sub>3</sub> and 600 nm from Mn until now. Son *et.al.* developed the Mn doping method via the addition of HBr.[40] However, the introduction of HBr modifies the CsPbBr<sub>3</sub> PL mechanism, leading to the presence of Mn PL.

Energy transfer from CsPbBr<sub>3</sub> affected by the HBr amount is investigated by PL and TRPL spectra (Fig. 4). Figure 4a shows the integrated PL peak area ratios of Mn (600 nm) to CsPbBr<sub>3</sub> (433 nm) obtained from figure 3c-g. The ratio increases from 1.27 to 1.99 as the HBr amount increases from 0.2 to 0.6 mL, indicating the increased Mn PL intensity relative to CsPbBr<sub>3</sub> PL. The ratio decreases to 1.22 as the HBr amount further increases to 1 mL, leading to the production of a maximum ratio of 1.99 for S5. TRPL data of S2-S7 monitored at 433 nm are shown in figure S4. All the lifetime decay curves can be fitted by biexponential function.

Table 2 the lifetime fitting results of S2-S7 monitored at 433 nm

	S2	S3	S4	S5	<b>S6</b>	S7
T1 (ns)	1.78	9.88	8.89	6.51	3.57	2.41
T2 (ns)	195.27	56.28	47.70	40.64	19.27	20.01
B1	0.13	0.53	0.59	0.72	0.52	0.64
B2	0.87	0.47	0.41	0.28	0.48	0.36

The fitting parameters are listed in table 2. The long lifetime is attributed to PbBr<sub>6</sub> octahedra structures, which is equivalent to the band edge recombination of CsPbBr<sub>3</sub> nanocrystals. Usually, the band edge recombination is associated to the emission of ~500 nm. In our case, the emission position is 433 nm. We believe it is associated with the PbBr<sub>6</sub> octahedra structures. Therefore, the long lifetime is attributed to this PbBr<sub>6</sub> octahedra structures. The short lifetime is ascribed to the surface recombination. Figure 4b shows the long lifetime of S2-S7. It is observed that the lifetime decreases from 195.3 ns to 20 ns as the HBr amount increases from 0.2 mL to 1 mL, indicating the energy transfer from CsPbBr<sub>3</sub> to Mn. The variation of the short lifetime within 10 ns is attributed to the nanoparticle surface including the surface defects and surface ligands (Fig. 4c). The energy transfer efficiency in S3-S7 from CsPbBr<sub>3</sub> to Mn is calculated by the equation of η=( T2<sub>S2</sub>-T2<sub>S3</sub>-7)/T2<sub>S2</sub>. The energy transfer efficiency increases with the increase of the amount of HBr (Fig. 4d).

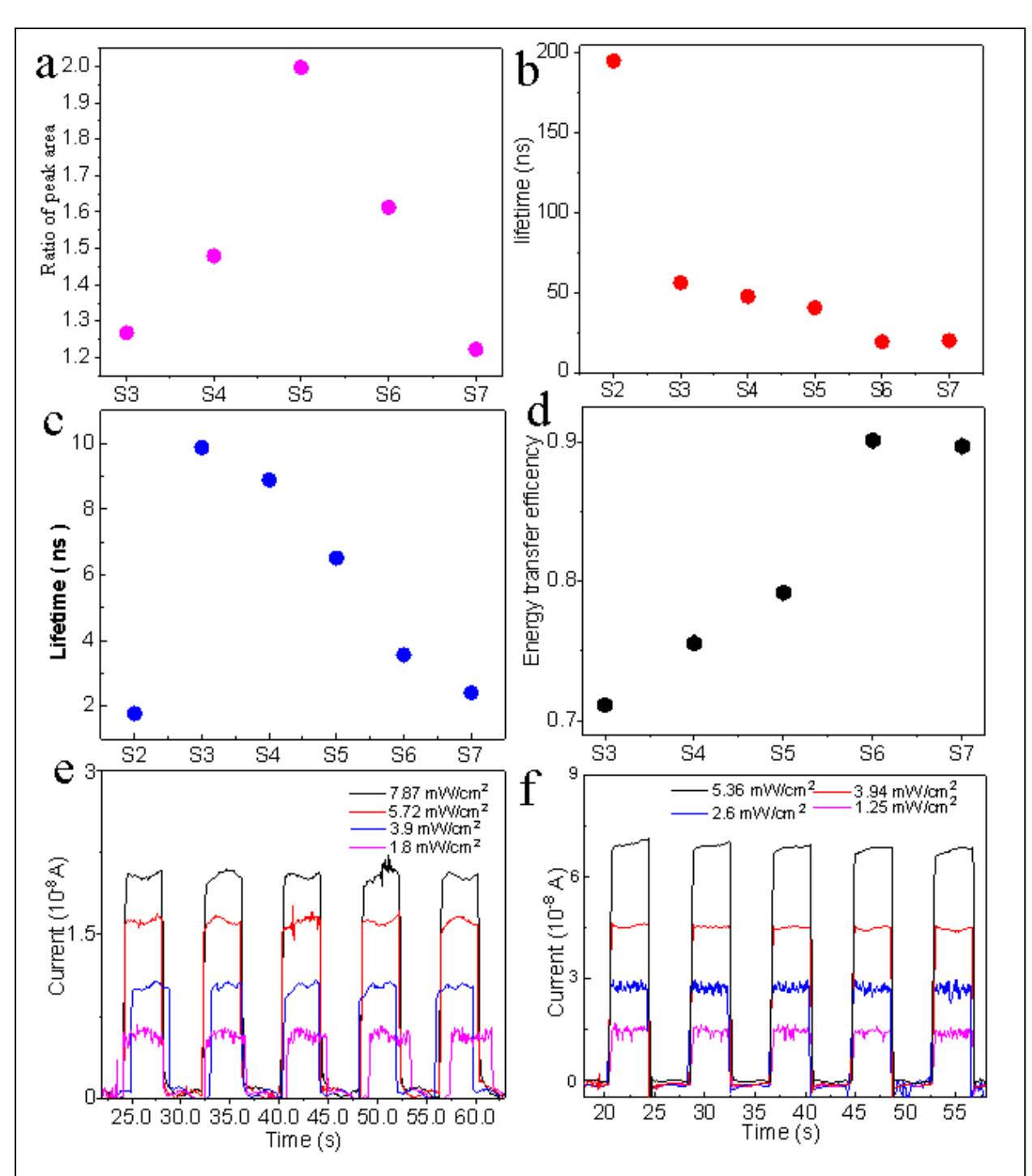


Figure 4 a PL peak area ratio of Mn and CsPbBr<sub>3</sub>. b Long lifetime values of CsPbBr<sub>3</sub> emission ( $\lambda_{em}$ =433 nm) of S2-S7. c short lifetime values of CsPbBr<sub>3</sub> emission ( $\lambda_{em}$ =433 nm) of S2-S7. d calculated energy transfer from CsPbBr<sub>3</sub> to Mn. d performance of photodetectors based on CsPbBr<sub>3</sub> (e) and CsPbBr<sub>3</sub>:Mn (f).

It reaches ~90% as the HBr amount is 0.8 mL and 1 mL for S6-S7. Therefore, the energy transfer efficiency is confirmed for S3-S7. The photodetectors based on the CsPbBr<sub>3</sub> and CsPbBr<sub>3</sub>:Mn with a structure of FTO/TiO<sub>2</sub>/CsPbBr<sub>3</sub>/Spiro/Au are also fabricated and studied in this work. Figure 4 e and f show the photodetector performance of the devices based on S2 and S3, respectively. It can be observed that the photocurrent increases with the increasing light power. Higher intensity of the photocurrent is obtained by the devices based on the Mn doped CsPbBr<sub>3</sub> compared to that of the undoped CsPbBr<sub>3</sub>. The detailed values are listed in table S1. This can be explained by the improved crystallinity of the CsPbBr<sub>3</sub> nanocrystals due to Mn doping, which is similar to the results of Eu doping[44].

#### Conclusion

In this work, Mn doped CsPbBr<sub>3</sub> nanocrystals are synthesized by hot injection method in the presence of HBr. HBr is required to dope Mn in CsPbBr<sub>3</sub>. The PL mechanism is modified by HBr additive, leading to the PL peak shifts to 433 nm, which is not regular CsPbBr<sub>3</sub> PL (503 nm). Thus, energy transfer happens from irregular CsPbBr<sub>3</sub> to Mn. PL energy transfer is studied as a function of the amount of HBr in terms of energy transfer efficiency. Two energy transfer channels are proposed in this work. CsPbBr<sub>3</sub> matrix can absorb energy then transfer to Mn, leading to red emission of Mn. PbBr<sub>6</sub> octahedra structures absorption at 430 nm can also transfer energy to Mn, resulting in red emission of Mn. TRPL study confirms the energy transfer from PbBr<sub>6</sub> octahedra structures to Mn. The optimum amount of HBr is 0.6 ml for a high PL peak ratio of Mn to CsPbBr<sub>3</sub>. Another benefit of the Mn doping is the improved crystallinity, leading to improved photodetector device performance compared to undoped CsPbBr<sub>3</sub>. This work presents the energy transfer mechanism in CsPbBr<sub>3</sub>:Mn nanocrystals.

# Acknowledgment

This work is supported by NSF-PREM grant #DMR-1826886. The TRPL equipment used in this work is supported by National Science Foundation Research Initiation Award: Novel Perovskite Solar Cells Based on Interface Manipulation (Award#1900047). Dr. Jian Xiong is supported by the National Science Foundation under Grant No. 1757220. This work is also partially supported by NIH grant (1U54MD015929) by using Horiba fluoromax-4 Compact Spectrofluorometer to measure the PL of the samples. The XRD used in this work is supported by the U.S. Army Engineer Research and Development Center (W912HZ-16-2-0021).

All data generated or analysed during this study are included in this published article and its supplementary information files.

Conflict of Interest - The author(s) declare that they have no conflict of interest.

### Reference

- [1] H. Zhao, Z. Hu, L. Wei, P. Zeng, C. Kuang, X. Liu, S. Bai, F. Gao, M. Liu, Efficient and High-Luminance Perovskite Light-Emitting Diodes Based on CsPbBr3 Nanocrystals Synthesized from a Dual-Purpose Organic Lead Source, Small. 16 (2020) 2003939. https://doi.org/10.1002/smll.202003939.
- [2] S.K. Karunakaran, G.M. Arumugam, W. Yang, S. Ge, S.N. Khan, Y. Mai, X. Lin, G. Yang, Europium (II)-Doped All-Inorganic CsPbBr3 Perovskite Solar Cells with Carbon Electrodes, Solar RRL. 4 (2020) 2000390. https://doi.org/10.1002/solr.202000390.
- [3] H. Li, X. Liu, Q. Ying, C. Wang, W. Jia, X. Xing, L. Yin, Z. Lu, K. Zhang, Y. Pan, Z. Shi, L. Huang, D. Jia, Self-Assembly of Perovskite CsPbBr3 Quantum Dots Driven by a Photo-

- Induced Alkynyl Homocoupling Reaction, Angewandte Chemie. 132 (2020) 17360–17366. https://doi.org/10.1002/ange.202004947.
- [4] Y. Ren, N. Zhang, Z. Arain, M. Mateen, J. Chen, Y. Sun, Z. Li, Polymer-induced lattice expansion leads to all-inorganic CsPbBr3 perovskite solar cells with reduced trap density, Journal of Power Sources. 475 (2020) 228676. https://doi.org/10.1016/j.jpowsour.2020.228676.
- [5] J. Ryu, S. Yoon, S. Lee, D. Lee, B. Parida, H.W. Kwak, D.-W. Kang, Improving photovoltaic performance of CsPbBr3 perovskite solar cells by a solvent-assisted rinsing step, Electrochimica Acta. 368 (2021) 137539. https://doi.org/10.1016/j.electacta.2020.137539.
- [6] D. Wang, W. Li, Z. Du, G. Li, W. Sun, J. Wu, Z. Lan, Highly Efficient CsPbBr3 Planar Perovskite Solar Cells via Additive Engineering with NH4SCN, ACS Appl. Mater. Interfaces. 12 (2020) 10579–10587. https://doi.org/10.1021/acsami.9b23384.
- [7] S. Wang, W. Shen, Y. Chu, W. Zhang, L. Hong, A. Mei, Y. Rong, Y. Tang, Y. Hu, H. Han, Mesoporous-Carbon-Based Fully-Printable All-Inorganic Monoclinic CsPbBr3 Perovskite Solar Cells with Ultrastability under High Temperature and High Humidity, J. Phys. Chem. Lett. 11 (2020) 9689–9695. https://doi.org/10.1021/acs.jpclett.0c02739.
- [8] Y. Haruta, T. Ikenoue, M. Miyake, T. Hirato, One-Step Coating of Full-Coverage CsPbBr3 Thin Films via Mist Deposition for All-Inorganic Perovskite Solar Cells, ACS Appl. Energy Mater. (2020). https://doi.org/10.1021/acsaem.0c01985.
- [9] C.-S. Jo, K. Noh, S.H. Noh, H. Yoo, Y. Kim, J. Jang, H.H. Lee, Y.-J. Jung, J.-H. Lee, J. Han, J. Lim, S.-Y. Cho, Solution-Processed Fabrication of Light-Emitting Diodes Using CsPbBr3 Perovskite Nanocrystals, ACS Appl. Nano Mater. (2020). https://doi.org/10.1021/acsanm.0c02334.
- [10] Y. Duan, C. Ezquerro, E. Serrano, E. Lalinde, J. García-Martínez, J.R. Berenguer, R.D. Costa, Meeting High Stability and Efficiency in Hybrid Light-Emitting Diodes Based on SiO2/ZrO2 Coated CsPbBr3 Perovskite Nanocrystals, Advanced Functional Materials. 30 (2020) 2005401. https://doi.org/10.1002/adfm.202005401.
- [11] X. Wang, S. Abbasi, D. Zhang, J. Wang, Y. Wang, Z. Cheng, H. Liu, W. Shen, Electrochemical Deposition of CsPbBr3 Perovskite for Photovoltaic Devices with Robust Ambient Stability, ACS Appl. Mater. Interfaces. 12 (2020) 50455–50463. https://doi.org/10.1021/acsami.0c14816.
- [12] J. Pradhan, P. Moitra, Umesh, B. Das, P. Mondal, G.S. Kumar, U.K. Ghorai, S. Acharya, S. Bhattacharya, Encapsulation of CsPbBr3 Nanocrystals by a Tripodal Amine Markedly Improves Photoluminescence and Stability Concomitantly via Anion Defect Elimination, Chem. Mater. 32 (2020) 7159–7171. https://doi.org/10.1021/acs.chemmater.0c00385.
- [13] V.M. Burlakov, Y. Hassan, M. Danaie, H.J. Snaith, A. Goriely, Competitive Nucleation Mechanism for CsPbBr3 Perovskite Nanoplatelet Growth, J. Phys. Chem. Lett. 11 (2020) 6535–6543. https://doi.org/10.1021/acs.jpclett.0c01794.
- [14] E.J. Lee, D.-H. Kim, R.P.H. Chang, D.-K. Hwang, Induced Growth of CsPbBr3 Perovskite Films by Incorporating Metal Chalcogenide Quantum Dots in PbBr2 Films for Performance Enhancement of Inorganic Perovskite Solar Cells, ACS Appl. Energy Mater. 3 (2020) 10376–10383. https://doi.org/10.1021/acsaem.0c01152.
- [15] L.A.B. Marçal, E. Oksenberg, D. Dzhigaev, S. Hammarberg, A. Rothman, A. Björling, E. Unger, A. Mikkelsen, E. Joselevich, J. Wallentin, In Situ Imaging of Ferroelastic Domain

- Dynamics in CsPbBr3 Perovskite Nanowires by Nanofocused Scanning X-ray Diffraction, ACS Nano. 14 (2020) 15973–15982. https://doi.org/10.1021/acsnano.0c07426.
- [16] B. Zhang, L. Goldoni, C. Lambruschini, L. Moni, M. Imran, A. Pianetti, V. Pinchetti, S. Brovelli, L. De Trizio, L. Manna, Stable and Size Tunable CsPbBr3 Nanocrystals Synthesized with Oleylphosphonic Acid, Nano Lett. 20 (2020) 8847–8853. https://doi.org/10.1021/acs.nanolett.0c03833.
- [17] K. Su, G.-X. Dong, W. Zhang, Z.-L. Liu, M. Zhang, T.-B. Lu, In Situ Coating CsPbBr3 Nanocrystals with Graphdiyne to Boost the Activity and Stability of Photocatalytic CO2 Reduction, ACS Appl. Mater. Interfaces. 12 (2020) 50464–50471. https://doi.org/10.1021/acsami.0c14826.
- [18] S. Wang, L. Du, Z. Jin, Y. Xin, H. Mattoussi, Enhanced Stabilization and Easy Phase Transfer of CsPbBr3 Perovskite Quantum Dots Promoted by High-Affinity Polyzwitterionic Ligands, J. Am. Chem. Soc. 142 (2020) 12669–12680. https://doi.org/10.1021/jacs.0c03682.
- [19] D. Vila-Liarte, M.W. Feil, A. Manzi, J.L. Garcia-Pomar, H. Huang, M. Döblinger, L.M. Liz-Marzán, J. Feldmann, L. Polavarapu, A. Mihi, Templated-Assembly of CsPbBr3 Perovskite Nanocrystals into 2D Photonic Supercrystals with Amplified Spontaneous Emission, Angewandte Chemie International Edition. 59 (2020) 17750–17756. https://doi.org/10.1002/anie.202006152.
- [20] Z. Bao, H.-D. Chiu, W. Wang, Q. Su, T. Yamada, Y.-C. Chang, S. Chen, Y. Kanemitsu, R.-J. Chung, R.-S. Liu, Highly Luminescent CsPbBr3@Cs4PbBr6 Nanocrystals and Their Application in Electroluminescent Emitters, J. Phys. Chem. Lett. 11 (2020) 10196–10202. https://doi.org/10.1021/acs.jpclett.0c03142.
- [21] M.J. Crane, L.M. Jacoby, T.A. Cohen, Y. Huang, C.K. Luscombe, D.R. Gamelin, Coherent Spin Precession and Lifetime-Limited Spin Dephasing in CsPbBr3 Perovskite Nanocrystals, Nano Lett. 20 (2020) 8626–8633. https://doi.org/10.1021/acs.nanolett.0c03329.
- [22] X. Cao, G. Zhang, Y. Cai, L. Jiang, W. Yang, W. Song, X. He, Q. Zeng, Y. Jia, J. Wei, Sustainable solvent system for processing CsPbBr3 films for solar cells via an anomalous sequential deposition route, Green Chemistry. (2020). https://doi.org/10.1039/D0GC02892D.
- [23] S.M.H. Qaid, H.M. Ghaithan, B.A. Al-Asbahi, A. Alqasem, A.S. Aldwayyan, Fabrication of Thin Films from Powdered Cesium Lead Bromide (CsPbBr3) Perovskite Quantum Dots for Coherent Green Light Emission, ACS Omega. 5 (2020) 30111–30122. https://doi.org/10.1021/acsomega.0c04517.
- [24] Q. Zhou, J. Duan, X. Yang, Y. Duan, Q. Tang, Interfacial Strain Release from the WS2/CsPbBr3 van der Waals Heterostructure for 1.7 V Voltage All-Inorganic Perovskite Solar Cells, Angewandte Chemie. 132 (2020) 22181–22185. https://doi.org/10.1002/ange.202010252.
- [25] Q. Shang, M. Li, L. Zhao, D. Chen, S. Zhang, S. Chen, P. Gao, C. Shen, J. Xing, G. Xing, B. Shen, X. Liu, Q. Zhang, Role of the Exciton–Polariton in a Continuous-Wave Optically Pumped CsPbBr3 Perovskite Laser, Nano Lett. 20 (2020) 6636–6643. https://doi.org/10.1021/acs.nanolett.0c02462.
- [26] C.H. Kang, I. Dursun, G. Liu, L. Sinatra, X. Sun, M. Kong, J. Pan, P. Maity, E.-N. Ooi, T.K. Ng, O.F. Mohammed, O.M. Bakr, B.S. Ooi, High-speed colour-converting photodetector with all-inorganic CsPbBr 3 perovskite nanocrystals for ultraviolet light

- communication, Light: Science & Applications. 8 (2019) 94. https://doi.org/10.1038/s41377-019-0204-4.
- [27] K.-K. Liu, Q. Liu, D.-W. Yang, Y.-C. Liang, L.-Z. Sui, J.-Y. Wei, G.-W. Xue, W.-B. Zhao, X.-Y. Wu, L. Dong, C.-X. Shan, Water-induced MAPbBr 3 @PbBr(OH) with enhanced luminescence and stability, Light: Science & Applications. 9 (2020) 44. https://doi.org/10.1038/s41377-020-0283-2.
- [28] S. Lin, H. Lin, C. Ma, Y. Cheng, S. Ye, F. Lin, R. Li, J. Xu, Y. Wang, High-security-level multi-dimensional optical storage medium: nanostructured glass embedded with LiGa 5 O 8: Mn 2+ with photostimulated luminescence, Light: Science & Applications. 9 (2020) 22. https://doi.org/10.1038/s41377-020-0258-3.
- [29] I. Antony K. J., D. Jana, Stable Mn-Doped CsPbCl3 Nanocrystals inside Mesoporous Alumina Films for Display and Catalytic Applications, ACS Appl. Nano Mater. 3 (2020) 2941–2951. https://doi.org/10.1021/acsanm.0c00213.
- [30] P. Song, B. Qiao, D. Song, J. Cao, Z. Shen, Z. Xu, S. Zhao, S. Wageh, A. Al-Ghamdi, Modifying the Crystal Field of CsPbCl3:Mn2+ Nanocrystals by Co-doping to Enhance Its Red Emission by a Hundredfold, ACS Appl. Mater. Interfaces. 12 (2020) 30711–30719. https://doi.org/10.1021/acsami.0c07655.
- [31] Q. Liu, K. Liu, Y. Liang, J. Sun, L. Dong, C.-X. Shan, Gram-scale and solvent-free synthesis of Mn-doped lead halide perovskite nanocrystals, Journal of Alloys and Compounds. 815 (2020) 152393. https://doi.org/10.1016/j.jallcom.2019.152393.
- [32] K. Xing, X. Yuan, Y. Wang, J. Li, Y. Wang, Y. Fan, L. Yuan, K. Li, Z. Wu, H. Li, J. Zhao, Improved Doping and Emission Efficiencies of Mn-Doped CsPbCl3 Perovskite Nanocrystals via Nickel Chloride, J. Phys. Chem. Lett. 10 (2019) 4177–4184. https://doi.org/10.1021/acs.jpclett.9b01588.
- [33] Y. Wang, S. Cao, J. Li, H. Li, X. Yuan, J. Zhao, Improved ultraviolet radiation stability of Mn2+-doped CsPbCl3 nanocrystals via B-site Sn doping, CrystEngComm. 21 (2019) 6238–6245. https://doi.org/10.1039/C9CE01150A.
- [34] F. Sui, M. Pan, Z. Wang, M. Chen, W. Li, Y. Shao, W. Li, C. Yang, Quantum yield enhancement of Mn-doped CsPbCl3 perovskite nanocrystals as luminescent down-shifting layer for CIGS solar cells, Solar Energy. 206 (2020) 473–478. https://doi.org/10.1016/j.solener.2020.05.070.
- [35] J. Ren, X. Zhou, Y. Wang, Water triggered interfacial synthesis of highly luminescent CsPbX3:Mn2+ quantum dots from nonluminescent quantum dots, Nano Res. 13 (2020) 3387–3395. https://doi.org/10.1007/s12274-020-3026-z.
- [36] M.C. De Siena, D.E. Sommer, S.E. Creutz, S.T. Dunham, D.R. Gamelin, Spinodal Decomposition During Anion Exchange in Colloidal Mn2+-Doped CsPbX3 (X = Cl, Br) Perovskite Nanocrystals, Chem. Mater. 31 (2019) 7711–7722. https://doi.org/10.1021/acs.chemmater.9b02646.
- [37] H. Yang, W. Fan, K. Hills-Kimball, O. Chen, L.-Q. Wang, Introducing Manganese-Doped Lead Halide Perovskite Quantum Dots: A Simple Synthesis Illustrating Optoelectronic Properties of Semiconductors, J. Chem. Educ. 96 (2019) 2300–2307. https://doi.org/10.1021/acs.jchemed.8b00735.
- [38] Y. Zhao, X. Zhang, C. Xie, W. Shi, P. Yang, S.P. Jiang, Controlling Mn Emission in CsPbCl3 Nanocrystals via Ion Exchange toward Enhanced and Tunable White Photoluminescence, J. Phys. Chem. C. 124 (2020) 27032–27039. https://doi.org/10.1021/acs.jpcc.0c08378.

- [39] Reversible Color Switching in Dual-Emitting Mn(II)-Doped CsPbBr3 Perovskite Nanorods: Dilution versus Evaporation | ACS Energy Letters, (n.d.). https://pubs.acs.org/doi/abs/10.1021/acsenergylett.9b01702 (accessed December 9, 2020).
- [40] D. Parobek, Y. Dong, T. Qiao, D.H. Son, Direct Hot-Injection Synthesis of Mn-Doped CsPbBr3 Nanocrystals, Chem. Mater. 30 (2018) 2939–2944. https://doi.org/10.1021/acs.chemmater.8b00310.
- [41] Y. Bekenstein, B.A. Koscher, S.W. Eaton, P. Yang, A.P. Alivisatos, Highly Luminescent Colloidal Nanoplates of Perovskite Cesium Lead Halide and Their Oriented Assemblies, J. Am. Chem. Soc. 137 (2015) 16008–16011. https://doi.org/10.1021/jacs.5b11199.
- [42] M. Liu, Z. Li, W. Zheng, L. Kong, L. Li, Improving the Stability of CsPbBr3 Perovskite Nanocrystals by Peroxides Post-treatment, Front. Mater. 6 (2019). https://doi.org/10.3389/fmats.2019.00306.
- [43] L. Zhang, Y. Zhang, W. He, H. Peng, Q. Dai, CsPbBr3 perovskite nanowires and their optical properties, Optical Materials. 109 (2020) 110399. https://doi.org/10.1016/j.optmat.2020.110399.
- [44] S.K. Karunakaran, G.M. Arumugam, W. Yang, S. Ge, S.N. Khan, Y. Mai, X. Lin, G. Yang, Europium (II)-Doped All-Inorganic CsPbBr3 Perovskite Solar Cells with Carbon Electrodes, Solar RRL. 4 (2020) 2000390. https://doi.org/10.1002/solr.202000390.

# **Supporting information:**

# Luminescence Properties of CsPbBr3:Mn

# Nanocrystals

Wencai He, Qiqi Zhang, Yifang Qi, Jian Xiong, Paresh Ray, Nihar Ranjan Pradhan, Tigran V.

Shahbazyan, Fengxiang Han, and Qilin Dai\*

Department of Chemistry, Physics, and Atmospheric Sciences, Jackson State University, Jackson, MS, 39217, United States

\*corresponding author: <a href="mailto:qilin.dai@jsums.edu">qilin.dai@jsums.edu</a>

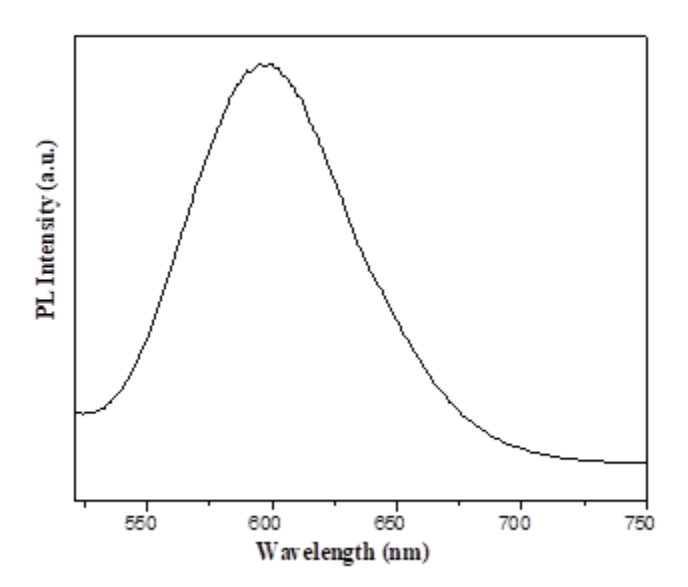


Figure S1 the PL spectra of S3 under the excitation of 433 nm

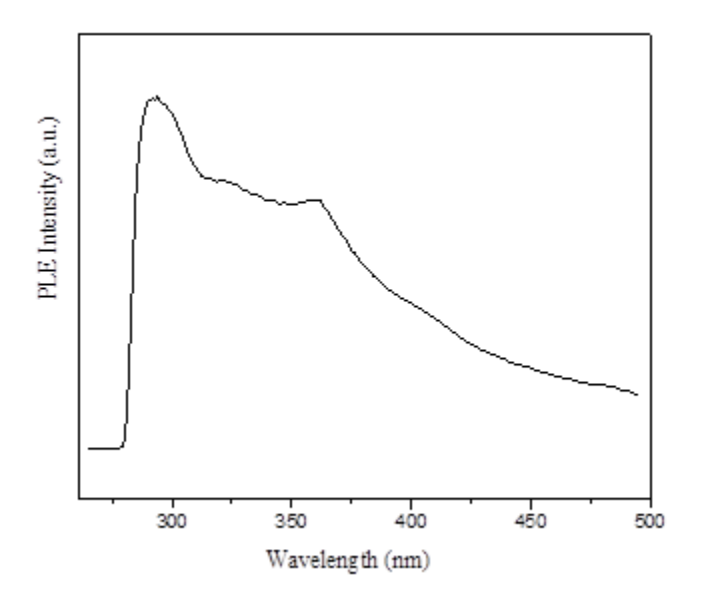


Figure S2 PLE spectrum of S1

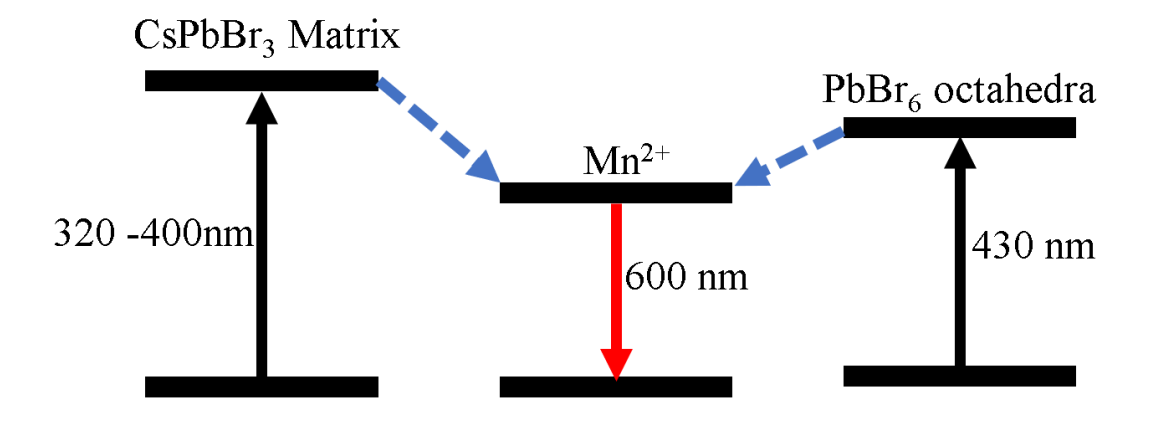


Figure S3 the energy transfer mechanism of CsPbBr<sub>3</sub>:Mn nanocrystals

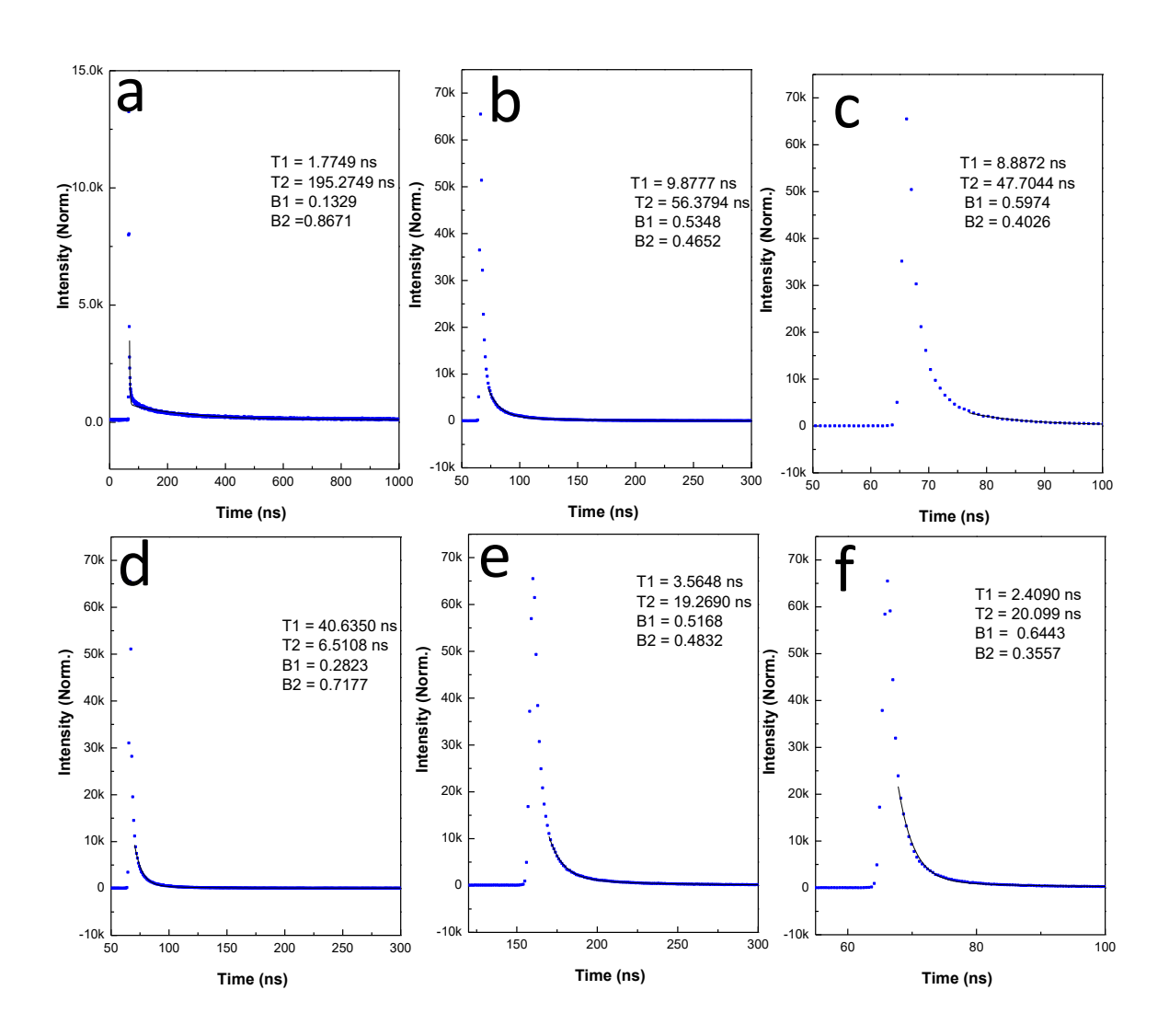


Figure S4 a-f TRPL spectra of S2-S7

Table S1 the photocurrent values of CsPbBr<sub>3</sub> nanocrystals. The light intensity in the brackets are the values used to measure the performance of the devices based on Mn doped CsPbBr<sub>3</sub>.

Light intensity (mW/cm²)	1.8 (1.25)	3.9 (3.94)	5.72 (2.6)	7.87 (5.36)
Photocurrent CsPbBr <sub>3</sub> (10 <sup>-8</sup> A)	0.6	1	1.65	2
Photocurrent CsPbBr <sub>3</sub> :Mn (10 <sup>-8</sup> A)	1.5	2.8	4.5	6.9